Vegetation Cover Change Associated With Changes in Hydro-Climatic Variables in Northern Sub-Saharan Africa in Recent Decades.

Faustin Katchele Ogou

CAS Key Laboratory of Regional Climate-Environment for Temperate East Asia, Institute of Atmospheric Physics, Chinese Academy of Sciences

Tertsea Igbawua (talk2tertsee@yahoo.com)

Federal University of Agriculture Makurdi https://orcid.org/0000-0002-5131-1445

Research Article

Keywords: Climate change, NDVI classification, Trends, Mann-Kendall, Northern Sub-Saharan Africa

Posted Date: October 27th, 2021

DOI: https://doi.org/10.21203/rs.3.rs-796485/v1

Vegetation cover change associated with changes in hydro-climatic variables in northern Sub-Saharan Africa in recent decades.

Faustin Katchele Ogou [1,2], Tertsea Igbawua [2,3]

[1]CAS Key Laboratory of Regional Climate-Environment for Temperate East Asia, Institute of Atmospheric Physics, Chinese Academy of Sciences, Beijing 100029, China

[2]University of Chinese Academy of Sciences, Beijing 100049, China

[3]Federal University of Agriculure, Makurdi, Benue State, Nigeria

Coressponding Author: Tertsea Igbawua; Email: tertsea.igbawua@uam.edu.ng

Abstracts

The environmental change in Northern Sub-Saharan Africa (NSSA) remains a challenge in relation with hydro-climatic variations and the low adaptation capacity of the region. The present study investigates the vegetation cover (NDVI) change associated with variations in hydro-climatic indicators over the period 1982 -2015. The conventional statistical techniques such as the linear and multiple regressions, Mann-Kendall test, Sen'slope and the Pearson's correlation were employed. The vegetation cover based on vegetation (NDVI) and hydro-climatic data were used. Trends in vegetation cover and hydro-climatic variables had monotonically increased except for the soil moisture that had monotonically decreased in the region. The proportion of significant positive (negative) changes were 46.78% (8.10%), 38.13% (0.34%), 52.12% (0.10%), 82.86% (0.00%) and 10.54% (38.27%) for NDVI, precipitation, potential evapotranspiration, temperature and soil moisture, respectively. The low vegetation dominated the NSSA region with a proportion of about 32% of the total area coverage. The vegetation classes including low coverage, very high coverage, and extreme high coverage exhibited increasing trends. Meanwhile, moderate coverage and high coverage exhibited decreasing trends. The area-averaged precipitation and temperature were positively correlated with the NDVI; however, the area-averaged soil moisture showed negative association with NDVI. Except the precipitation and Significant positive (negative) correlations of NDVI with the precipitation, temperature and soil moisture at the 5% level occupied 1.67% (11.59%), 3.37%(26.19%) and 10.24% (6.75%), respectively. However, the combine effects of hydro-climatic variables are better for the monitoring of vegetation cover. This confirms that the vegetation cover is influenced by many factors.

Keywords: Climate change, NDVI classification, Trends, Mann-Kendall, Northern Sub-Saharan Africa

1. Introduction

The climatological disasters notably, droughts, have caused many fatalities in the Eastern part of Africa with more than one-third of the population affected in Djibouti, Eritrea and Somalia followed by West and South Africa (Lukamba, 2010). These events have affected undoubtedly the ecosystems of the area as well as the water resources (Vlek et al., 2008). Several studies have paid attention to the dynamical change of ecosystems nowadays (Bachelet et al. 2001; Traore et al. 2014; Xu, Yang, and Chen 2016; Zhang et al. 2016; Pei et al. 2018). NDVI has been one of the variables used widely to characterize the ecosystem and land cover at the annual and interannual time scales (Barbosa et al., 2006; Dardel et al., 2014; Pravalie et al., 2014). A particular interest exists in studying the impacts of climate change on agriculture in Sub-Saharan Africa, and on vital investments to support an adjustment to climate fluctuations (Schlenker and Lobell, 2010). Until now, the scientific basis for appraising production risks and adjustments of investments have been somewhat limited (Schlenker and Lobell, 2010). The interannual and intraseasonal variability of vegetation index revealed a robust photosynthetic activity over the Sahel, which was interrelated to above-normal convection and rainfall within the intertropical convergence zone (ITCZ) in the summertime (Philippon et al., 2007). It was also associated partly with colder (warmer) SST in the eastern tropical Pacific (the Mediterranean) (Philippon et al., 2007). Previous studies have investigated the relationship between climate factors and the Normalized Difference Vegetation Index (NDVI) and found that precipitation and soil moisture, temperature somehow played a role in the greening of Sahel (Zhang et al. 2005; Olsson, Eklundh, and Ardö 2005; Bégué et al. 2011; Igbawua et al. 2016; Zewdie, Csaplovics, and Inostroza 2017; Leroux et al. 2017). However, the temporal coverage of the data available for these studies was short. For instance, over the NSSA, the precipitation behaved differently regarding the length of studied period (Ogou, 2019). A long-time period of NDVI data would be more helpful to identify departures in primary production for entire ecological zones, for instance, the Sahelian zone (Tucker, 1986). The NDVI calculation is expressed as the difference between red (RED) and near-infrared (NIR) reflectance with the following formula: $\mathrm{NDVI} = \frac{\mathrm{NIR}-\mathrm{RED}}{\mathrm{NIR}+\mathrm{RED}}$. A study has attributed the changes in the greenness observed over the sub-Saharan to climatic factor (e.g., rainfall) and non-climatic drivers (e.g., soil moisture) (Hoscilo et al., 2015). The climate and non-climatic factors that contribute to the sub-Saharan greenness are not fully studied.

A positive change in NDVI has been observed since 2002 according to earlier studies (Eklundh and Olsson, 2003), but the positive change proportion of NDVI was less than the demand in biomass of the area (Abdi et al., 2014). All the above mentioned authors highlighted that many variables contribute to change in NDVI over the region, however, the precipitation and soil moisture were the main focus. However the combination of multiple variables had not been studied yet.

The GIMMS improvement scheme through the Empirical Mode Decomposition (EMD) transformation method (Pinzon et al., 2005) implied that the GIMMS NDVI dataset is dynamic by nature and must be recalculated every time that more recent data are added (Fensholt and Proud, 2012). Henceforth, it is essential to investigate factors influencing vegetation growth regularly. Before analyzing the influence of climate change on NDVI, climate change is studied. These datasets are preferred because it is recommended 30-year period for a climatological study. At the global scale, the MODIS NDVI showed a good a good relationship with NDVI3g (Fensholt and Proud, 2012). Hence, the NDVI3g (NDVI) is used through this work.

To the knowledge of the authors, the classification of vegetation based on NDVI values has not yet been studied over the area, which is important to comprehend the vegetation dynamics. Moreover, the relationship of these classes with climate factors still uncovered. Furthermore, quantitive study of changes in these variables were not shown in recent decades. Therefore, the present paper aims at:

1) Classifying the vegetation cover based on the NDVI values
2) Reviewing the trends in hydro-climatic variables and NDVI and
3) Scrutinizing the relationship between NDVI and climate factors.

The results of the analysis will be important for land cover and land use management, monitoring of the hydro-climatic variables over the region.

2. Data and Methods

2.1.Study area

In order to give a sub-regional analysis of the climate and NDVI parameters, the NSSA region was divided as eastern Sahel (ES) (eastern Ethiopia), northern Sahel (NS), and the Guinea Coast (GC) and presented in Figure 1. The ES was seriously affected by recurrent, erratic rainfall and high and increasing of temperature conditions (Mulugeta et al., 2017). They also showed the

seasonality of rainfall over the region, which was from June to August. Wagner and da Silva (1994) argued that the rainfall regime in the NS was also featured by a boreal summer rainy season, but this season was shorter. The study reported that the NS rainfall was highly correlated with a pattern of positive SST anomalies in the North Atlantic and negative SST anomalies in the South Atlantic implying a positive meridional gradient near the Equator. The GC was the region receiving more rainfall compared with others regions. A positive relationship is found between the precipitation of this region and the southern oscillation Atlantic Ocean (Okoro et al., 1979). The period of more rainfall is from June to September (Wagner and da Silva, 1994).

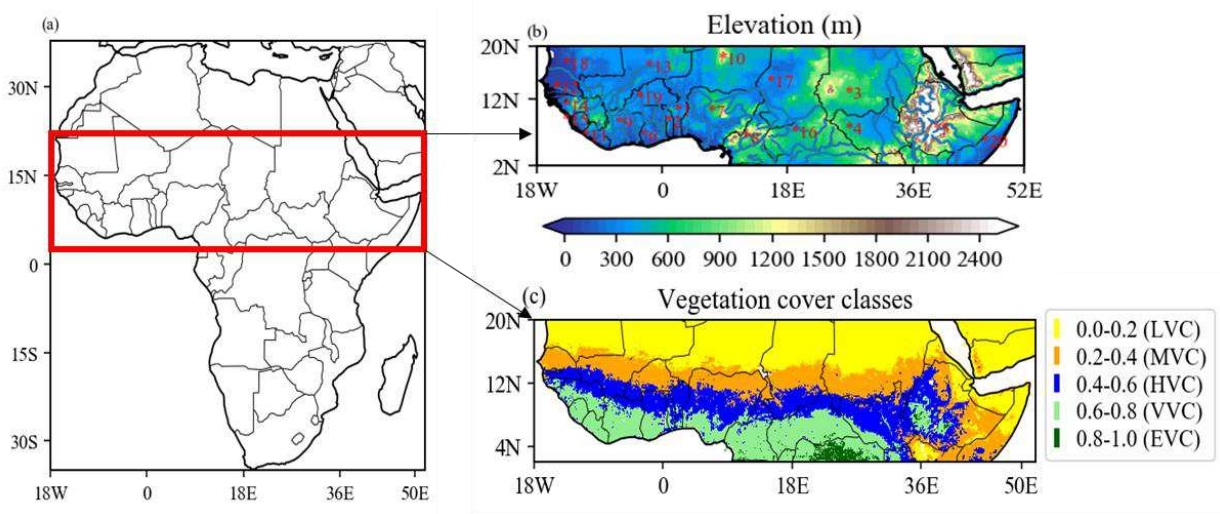

Fig. 1: (a) Map of Africa showing the study area in red rectangle, (b) the elevation and (c) the classification of vegetation cover based on NDVI values. The * with numbers in red represent countries (1 = Benin, 2 = Togo, 3 = Sudan, 4 = South-sudan, 5 = Ethiopia, 6 = Ghana, 7 = Nigeria, 8 = Cameroun, 9 = Ivory Coast, 10 = Niger, 11 = liberia, 12 = Senegal, 13 = Mali, 14 = Guinea, 15 = Sierra-Leone, 16 = Central African Republic, 17 = Chad, 18 = Mauritania, 19 = Burkina-Faso and 20 = Erithrea).

The distribution characteristizing the NDVI values in the NSSA was given in Figure 1 (b). NDVI's classes were defined as follows: 0.0−0.2, 0.2−0.4, 0.4−0.6, 0.6–0.8, and 0.8–1.0 for low vegetation coverage (LVC), moderate vegetation coverage (MVC), high vegetation coverage (HVC), very high vegetation coverage (VVC), and extreme high vegetation (EVC), respectively. Similar classification has been adopted by researchers to understand the dynamics of the vegetation cover (Peng, Kuang, & Tao, 2019; Yang et al., 2019).

2.2.Data

The high-resolution data of the world's meteorological stations over land areas are obtained from the Climatic Research Unit (CRU) of the University of East Anglia (Harris et al., 2014). The monthly precipitation (PRE), temperature (TMP) and potential evapotranspiration (PET) with a spatial resolution of 0.5°×0.5° (lon/lat) are used. The temporal coverage of the datasets is from 1901 to 2016 and they are freely available at the following link: https://crudata.uea.ac.uk/cru/data/hrg/cru_ts_4.01/cruts.1709081022.v4.01/.

The Climate Prediction Center (CPC) soil moisture data of a single column of depth 160 cm provided by NCEP Reanalysis data provided by the NOAA/OAR/ESRL PSD, Boulder, Colorado, USA, from their Web site at https://www.esrl.noaa.gov/psd/ (Dool, 2003) was used. The temporal coverage of the data was from 1948 to near present at the spatial resolution of 0.5°×0.5°.

Likewise, we collected the normalized difference vegetation index (NDVI) data sets from https://ecocast.arc.nasa.gov/data/pub/gimms/3g.v1/, which has a horizontal resolution of 1/12º×1/12º and a temporal spanning from 1981 to 2015 (Pinzon and Tucker, 2014). The Dataset was generated from the Advanced Very High-Resolution Radiometers (AVHRR) Global Inventory Modelling and Mapping Studies (GIMMS) third generation (NDVI) using an Artificial Neural Network derived model.The NDVI is used because of it has the longest time spanning, which more suitable for climate analysis and as proxy for vegetation greenness (Herrmann et al., 2005).

2.3.Methods

The original NDVI resolution has been up scaled to 0.5°×0.5° using the arithmetic means of six by six windows to match the resolution of hydro-climatic datasets(Zhang, Wu, Yan, & Chen, 2017) to evaluatethe relationship between climate factors and vegetation cover.The non-vegetation cover area (i.e., NDVI <= 0) was masked out before the analysis.

The term correlation used in statistics described a linear statistical relationship between two random variables. Before investigating the drivers of NDVI change, we conducted the test of collinearity between the climate factors using the variance inflation factor (VIF) and matrix

correlation (r). The stronger the relationshipis; the stronger the correlation is. The given formula is as follows:

$$r = \frac{\sum_{i=1}^{n}(X_i-\overline{X})(Y_i-\overline{Y})}{\sqrt{\sum_{i=1}^{n}(X-\overline{X})^2 * \sum_{i=1}^{n}(Y_i-\overline{Y})^2}} \quad (1)$$

Where X_i is the annual value of each variable, $\overline{X}$ ($\overline{Y}$) is the mean value of a variable in all years, Y_i is the annual of a climate factor (e.g., TMP, PRE, SM) in all years, n is the number of samples; r is the correlation coefficient between X_i and Y_i. The r is useful because it provides the degree of agreement between two variables.

The departures have been used to describe the regional climatic at global (Jones and Hulme, 1996), continent (Nicholson, 1980, 2000) and regional (Nicholson and Kim, 1997) scales. It should be mentioned that the missing values of each parameter were ignored in the calculation (they were ignored) processes.

$$\text{Std. Ano.} = \frac{X_i-\overline{X}}{\sigma} \quad (2)$$

Where X_i is the yearly dataset, $\bar{X}$is the time-mean of the whole area of the variable. Negative A indicates a decrease of variable and positive A indicates an increase in it. The equation is defined as:

$$\overline{X} = \frac{\sum_{i=1}^{n} X_i}{n} \quad (3)$$

Where n is the total number of data.The linear regression is expressed as follows:

$$Y_i = b_0 + bX_i + \varepsilon \quad (4)$$

Where the b_0 represents the constant (when b = 0), $\varepsilon$the residual error and b the regression coefficient. The regression coefficient equation is given:

$$b = \frac{n\times\sum_{n=1}^{n} X_i Y_i - \sum_{n=1}^{n} X_i \sum_{n}^{i=1} Y_i}{n\sum_{n=1}^{n} X_i^2 - (\sum_{n=1}^{n} X_i)^2} \quad (5)$$

Moreover, the multiple regression based on the ordinary Least square (OLS) was used. The following equation represents the multi-regression model:

$$\frac{NDVI_i-\overline{NDVI}}{\sigma_{NDVI}} = \beta_1 \frac{PRE_i-\overline{PRE}}{\sigma_{PRE}} + \beta_2 \frac{TMP_i-\overline{TMP}}{\sigma_{TMP}} + \beta_3 \frac{SM_i-\overline{SM}}{\sigma_{SM}} + \varepsilon \quad (6)$$

Where over-bar represents the mean over the whole area, $\beta_1, \beta_2, \beta_3$represent the slope, σ is the standard deviationand ε is the residual error of each variable. Furthermore, each variable was standardized to circumvent the problem of the units.

The Mann–Kendall (MK) test (Gilbert, 1987; Kendall, 1975; Mann, 1945) was applied to assess statistically the possible existence of a monotonic upward/downward tendency of the drought indicators. We applied the sequential MK technique to emphasize the abrupt change. The following formula is given for the MK trend analysis:

$$S = \sum_{i=1}^{n-1} \sum_{j=i+1}^{n} sign(x_j - x_i) \quad (7)$$

Where S is the statistical trend and,

$$sign(x) = \begin{cases} +1 \; if \; (x_j - x_i) > 0 \\ 0 \; if \; (x_j - x_i) = 0 \\ -1 \; if \; (x_j - x_i) < 0 \end{cases} \quad (8)$$

Where n is the length of the time series data set and xi … xj stand for the observations at times i to j, correspondingly. According to the hypothesis of independent and randomly distributed random variables, the S statistic is approximately normally distributed when n ≥ 8, as follows:

$$E(S) = 0 \quad (9)$$

$$V(S) = \frac{n(n-1)(2n+5) - \sum_{i=1}^{j} t_i(t_i-1)(2t_i+5)}{18} \quad (10)$$

Where j is the number of tied groups and t_i is the size of the ith tied group. As a result, the standardized Z (calculated in the case of MK) test statistics follow a normal standardized distribution:

$$Z = \begin{cases} \frac{S-1}{\sqrt{V(S)}} \; if \; S > 0 \\ 0 \; if \; S = 0 \\ \frac{S+1}{\sqrt{V(S)}} \; if \; S < 0 \end{cases} \quad (11)$$

A significance test is determined based on the result of the Z value. The sign of Z either positive or negative is indicating an upward or downward trend of the tested variable. Based on the outputs of the Z value, the trend is not rejected when the Z value is greater in absolute value than the critical value Zα, at a selected significance level of α. The Sen's non-parametric method was used to assess the slope magnitude in the variables (Here, drought indices). The slope (Tm) for all data pairs is calculated as (Sen, 1968):

$$T_m = \frac{x_j - x_k}{j-k}, m = 1,2,\ldots,m. \quad (12)$$

Where x_j and x_k are considered as data values at time j and k for j > k. If there are n values of x in the time series, we obtain as many as N = (n(n-1))/2 slope estimates of T_m The median of these N values of T is the Sen's estimator of slope ranked from the smallest to the largest which is given as:

$$T_i = \begin{cases} T_{\frac{N+1}{2}} & \text{if N is odd} \\ \frac{1}{2}\left(T_{\frac{\alpha}{2}} + T_{\frac{N+2}{2}}\right) & \text{if N is even} \end{cases} \quad (13)$$

3. Results

3.1.NDVI variation and its proportion

Figure 2 showed the monthly climatology of the NDVI in NSSA from 1982 to 2015. The NDVI decreased slightly from January to February where it reached its minimum. Nevertheless, from March to September, the vegetation has increased whereby; it reached a peak in September and gradually decreased from October to Decmber. The peak of the NDVI recorded in September was 0.41. In this study, the start of the season began in April and ended in November. Many studies used a similar technique to define the seasonality of climate variables (e.g., PRE, TMP, moisture budget) (Chou et al. 2009; Yang et al. 2013). A study over western Africa showed that fires had a profound influence on the composition of the present forest canopy (Swaine, 1992). The two months (i.e., January and February) corresponded to the harmattan (dry air) period and are dominated by the burning activities (bush fire). Therefore, high evapotranspiration due to high temperature and low precipitation induced the soil moisture-laden. These conditions could cause the low vegetation observed from January to February, in particular, the lowest value observed in February. The pattern of monthly NDVI dynamics obtained in our study was similar to that gotten in a previous study over the Guinea Coast (Aklesso et al., 2018), however, with different amplitude. The difference in amplitude could be investigated from spatial and temporal extents. According to Zhang et al. (2018), the weak value of NDVI in February was attributed to the decline in deciduous vegetation over his region of study. This reason could also be valuable for the NSSA region that was characterized by deciduous vegetation.

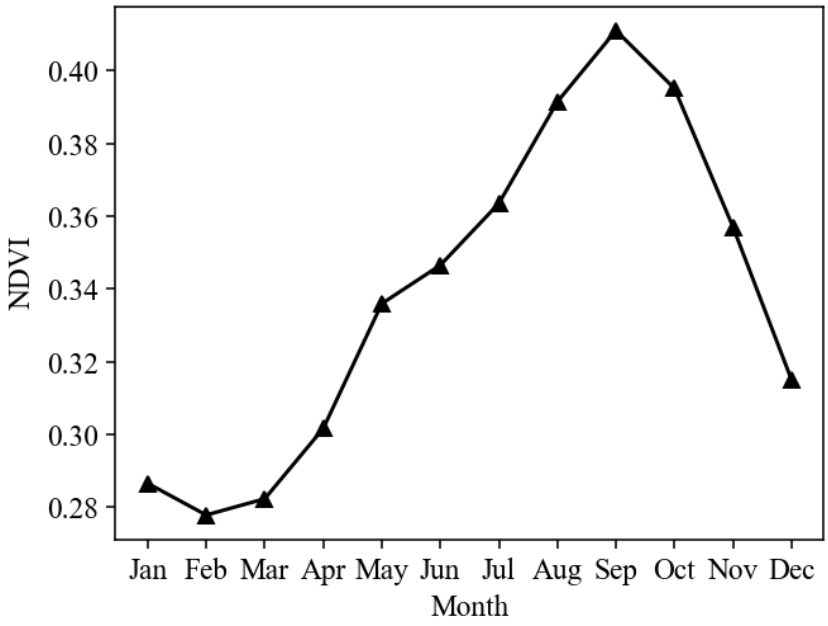

Fig. 2: Monthly Climatology of NDVI for the period 1982–2015.

The examination of the variation in NDVI was indispensable to comprehend the vegetation role in regional and global ecosystem stability (Gu et al., 2018). Hence, we investigated the change in vegetation cover based on the annual cycle. Figure 3 depicted the area percentage of each vegetation coverage class of annual NDVI. The classes of annual NDVI such as the LVC, MVC, HVC, VVC, and EVC occupied 32.02%, 18.37%, 17.08%, 14.77%, and 1.22%, respectively. From this result, the NSSA was dominated by sparse vegetation coverage, which is in line with the findings of Los, (2013).

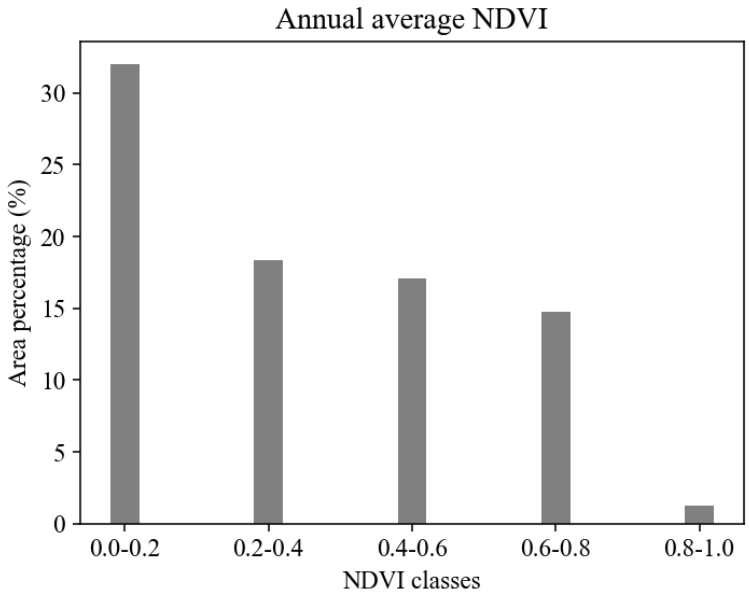

Fig. 3: Histogram of the area percentage of classes in NDVI for the period between 1982 and 2015.

3.2. Temporal trends in annual climate variables, annual NDVI, and the relationships between the sub-regions

The linear regression trend (Figure 4) and non-parametric trend (Figure S1) tests were used to show the tendency in hydro-climatic variables and the NDVI. The MK test was also applied to verify whether the tendency showed by linear trend is monotic. The relationships between the variations of climate factors of sub-regions were also assessed over the period 1982–2015 for NDVI, PRE, PET, TMP, and SM. This evaluation is important for facilitating the prediction and monitoring of sub-regions' climate conditions given that of the other. The sub-regions considered are northern Sub-Saharan Africa (NSSA), Guinea Coast (GC), Northern Sahel (NS), and eastern Sahel (ES). It can be seen that most regions experienced greening trends as depicted by the NDVI analysis (Figure 4(a)). The slope change rate in NDVI was 0.0005 $year^{-1}$, 0.0009 $year^{-1}$, 0.0001$year^{-1}$and over the NSSA, GC, and NS respectively, which were significant at the 5% level ($p < 0.05$). Approximately, for the NS area, a study by Kaspersen et al. (2011), has found a change rate of 0.0011 $year^{-1}$, which was not significant statistically. However, in the ES, the slope change rate in NDVI was 0.0001 $year^{-1}$ that was non-significant at the 5% level. The positive slope change rate meant the entire NSSA had experienced increased vegetation cover. Dardel et al., 2014 found that trends in NDVI were positive everywhere in Sahel over 1982−2011, which is in agreement

with our findings. The increase in NDVI has been interpreted as vegetation recovery from the Sahel drought (Herrmann et al., 2005; Olsson et al., 2005)

Figure 4 (b) showed that trends in NSSA, GC, NS were significant and positive during the period of the study. Slope change rates in PRE were 0.22 mm $year^{-1}$, 0.30 mm $year^{-1}$ and 0.15 mm $year^{-1}$ for the regions such as NSSA, GC, and NS, respectively. At this time, the trend in PRE over the ES was positive, but with a non-significant change rate. The change rate of PRE over the area (ES) was 0.05 mm $year^{-1}$. The positive change in the time series of NSSA indicated that the precipitation had increased over the area during the period of study.

Significant positive variation rates in PET were obtained over the NSSA (Figure 4(c)). Indeed, slope change values of 0.45 mm day^{-1} $year^{-1}$, 0.28 mm $day^{-1}year^{-1}$, 0.44 mm $day^{-1}year^{-1}$ and 1.39 mm $day^{-1}year^{-1}$ in PET were acquired in the NSSA, GC, NS and ES respectively that were significant at the 5% level. It can be seen that the ES experienced the highest change rate in PET, while the GC experienced the lowest in it. The positive change implied that PET had increased over the 1982–2015 time interval in the NSSA region.

Figure 4(d) displayed the slope change in TMP over 34 years. A significant positive change rate in TMP was evident with the values of 0.0265°C $year^{-1}$, 0.0234°C $year^{-1}$, 0.0314°C $year^{-1}$ and 0.0233°C $year^{-1}$for the NSSA, GC, NS and ES respectively. These signified that the entire NSSA was warming. Among these subdivisions, NS was the warmest area, while ES was the least warm area. The consistent increase of temperature could be attributed to elevated CO_2 emissions.

In Figure 4(e), SM exhibited downward tendencies in each of the four regions. Significant slope change values of −0.8819 mm $year^{-1}$, −1.5785 mm $year^{-1}$ over NSSA and GC were obtained in SM, respectively whereas insignificant slope change values of −0.1570 mm $year^{-1}$ and −0.0778 mm $year^{-1}$ over NS and ES were revealed, respectively. In general, a decrease in SM was evident during the study period in this region. The highest change rate in SM was observed over GC, while the lowest was observed in ES. The tendencies detected by the linear regression trend test as siginificant at the 5% level in hydro-climatic variables and NDVI are monotonic (Table S1). Slopes change rate

We also employed the Pearson correlation to examine the linkage between the sub-regions through the defined variables. The technique would show the confidence of the analysis over NSSA and its sub-regions (NS, GC, and ES), the confidence of association betweenclimate variables of the sub-regions. The regional interrelationship between NDVI and hydro-climatic

281 variables was analyzed for the period 1982−2015. The NDVI of NS correlated with the NDVI of
282 ES,but was found to be insignificant at the 5% level ($r = 0.31$, $p = 0.08$), whereas the NDVI of
283 remaining regions were significantly correlated with one another over the same period. It was
284 found that PRE of ES and that of the NSSA were not significantly interrelated at the 5% level. The
285 association coefficient of these two regions was significant at the 15% level ($r = 0.25$ and $p = 0.14$).
286 Non-significant correlations of the GC with the ES and that of NS with ES based on PRE at the
287 5% level were palpable. The association coefficients were 0.21 ($p = 0.22$) and 0.14 ($p = 0.42$),
288 respectively. The SM of GC correlated with the NDVI of ES was insignificant at the 5% level (r
289 $= 0.28$, $p = 0.09$), in contrast to remaining regions where significant relationships were observed
290 based on this variable. At this time, the associations of the variable over the GC with that of the
291 ES, GC with NS, NS with ES, NSSA with GC, NSSA with NS and NSSA with ES based on PET,
292 and TMP were significant at 5% level.

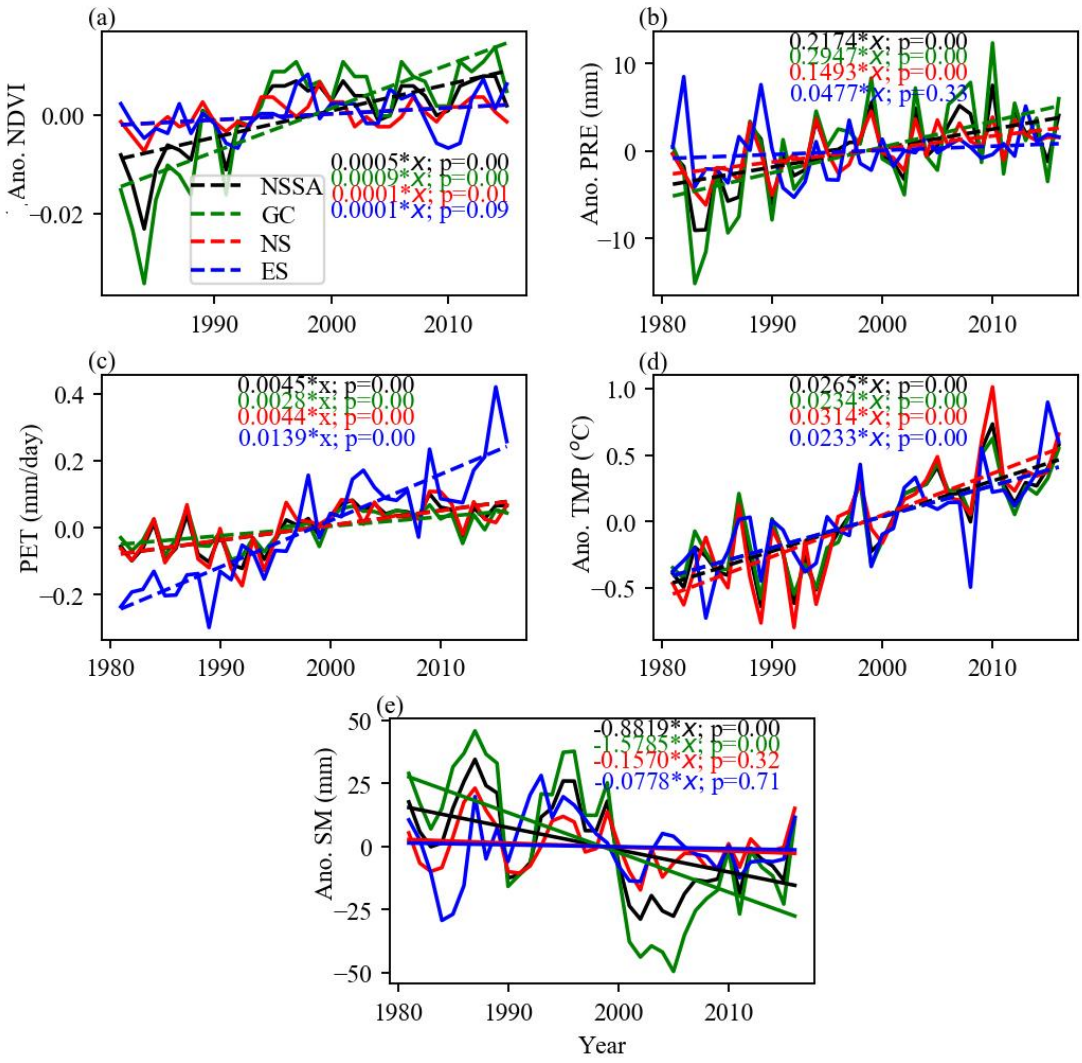

293

294 **Fig 4** : Temporal variations and its linear trends in (a) NDVI (1982–2015), (b) PRE, (c) PET, (d)
295 TMP and (e) SM (1981–2016) over the NSSA. Legends of the colors are indicated in (a).

296 **3.3.Temporal trends in annual NDVI classes**

297 The linear trend in the time series of the vegetation class was depicted in Figure 5. The
298 LVC, and HVC showed a weak upward and downward tendency with a value of 0.0036 ($p =$
299 0.84)and −0.0048 ($p = 0.43$), respectively. It meant that the low vegetation cover slowly
300 ameliorated over time while the moderate vegetation of the NSSA reduced slowly over the region.
301 Figure 5 (b) showed a decreasing trend in MVC with the change rate of −0.0447 ($p = 0.03$) that
302 was significant ($p < 0.05$),which translated into reduction in moderate vegetation cover. Many
303 factors such as soil water condition, modification of soil properties (Nicholson and Farrar, 1994)

or human activities (Spiekermann, Brandt, and Samimi, 2015) or natural condition as well as the precipitation variability could explain negative trends in these classes.

In Figure 5 (d), an upward tendency could be seen in VVC with a change rate of 0.0423 ($p = 0.00$) that was statistically significant ($p < 0.05$). That implied that very high vegetation cover had increased. A positive upward tendency was gotten from an EVC (Figure 5 (e)) with a non-significant change rate with a slope of 0.0013 ($p = 0.44$). The extreme vegetation cover had been weakly ameliorated over the region in the past 34 years. In contrast, Peng et al. (2019) found significant increasing trend in vegetation cover, which had a coverage index higher than 0.8.

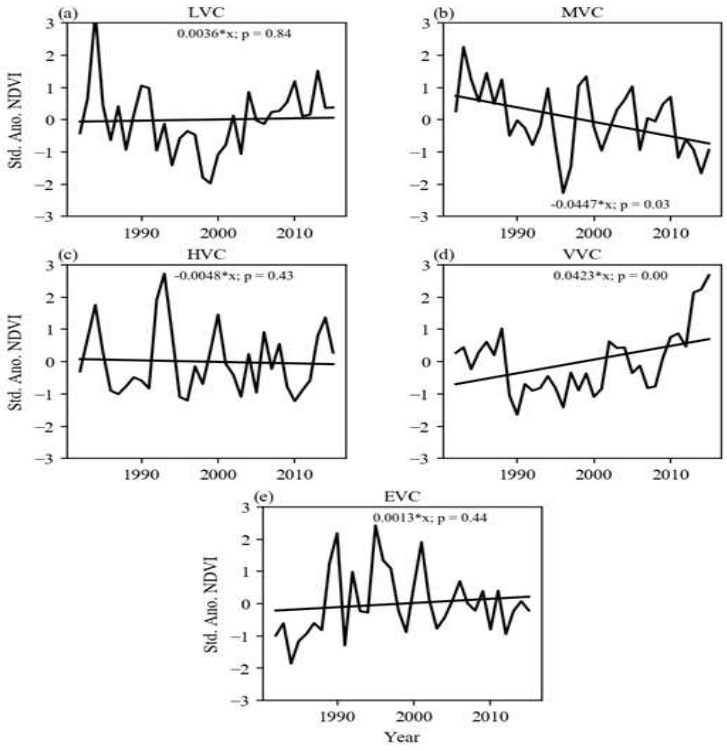

Fig. 5 : Variations in NDVI classes with its linear trends over the NSSA

3.4.Spatial distribution based on MK and linear trends of annual hydro-climatic and NDVI

The results of the MK trends (Figure 6) patterns are analyzed in this section due to its similarity with that of linear trends (Figure S1). Dominant positive changes of the NDVI could be observed over the NSSA (Figure 6 (a)). However, some locations showed adverse changes in NDVI, for example, part of eastern Mauritania, western Mali, southwestern and central eastern of Niger, eastern of Sudan and central Ethiopia. A significant change at a 5% level was evident over considerable parts of the area. The maximum and minimum slope change rates of NDVI for the

whole region were 0.81 and −0.78, respectively. Positive trends in NDVI occupied a proportion of 64.46%, whereas negative trends accounted for 19.40% of the total area. Among the proportion of positive (negative) trends in NDVI, 30.85% (3.91%) were significant at the 5% level, respectively.

Figure 6 (b) exhibited positive and negative changes in PRE during the period of study. Large areas of the NSSA experienced a positive change in PRE, whereas small areas of the region experienced an negative change in it. We observed a negative change in PRE over southeastern Nigeria, northwestern Cameroon and parts of Eritrea. The maximum and minimum slope change rate in PRE of the whole region was 0.56and −0.44respectively. The positive trend in PRE occupied a proportion of 78.15%, whereas 6.88% presented negative trends over the total area. Among the proportion of positive (negative) trends in PRE, 18.23% (0.14%) was significant, correspondingly.

The PET showed a significant positive trend (at the 5% level) over a considerable part of the area (Figure 6 (c)). Meanwhile, a small part of the area exhibited significant negative trends, presented for the regions of South Sudan, southwestern Niger, Mali, northernmost of Burkina-Faso, Ivory Coast, Ghana and eastern Guinea. The maximum and minimum slope change rates of the PET of the whole region were 0.78 and − 0.26, respectively. The positive trend in PET occupied a proportion of 76.41 %, whereas a proportion of 9.17 % revealed the negative trend in the total area. Among the proportion of positive (negative) trends in PET, 35.67% (0.00%) was significant, correspondingly.

Figure 6 (d) displayed the trend in TMP in NSSA. It could be seen that significant positive trends were dominated in the region. That meant that TMP had increased over the NSSA area during the last 34 years. The warming trend observed in TMP could be due to the increases in CO_2. However, the very weak decreasing tendency of TMP was observed over southeastern Sudan, Benin, Togo, eastern Ghana, western Nigeria and a noteworthy part of Mali. The lowest proportionof trends in TMP was 0.02%, whereas that of the highest was 85.93% of the total area. The maximum and minimum change rates in TMP were 0.16and 0.75, respectively. Among the proportion of positive (negative) trends in TMP, 75.99% (0.00%) was significant.

Heterogeneous trend patterns were observed in SM (Figure 6 (e)),implying that the regions within the NSSA experienced varying conditions (increasing or decreasing) of soil moisture. The proportion of negative trends in SM was 60.02%, whereas that of positive trends in SM was 26.23% of the total area. The maximum and minimum change rates in SM were 0.6and −1.00,

respectively. Among the proportion of positive (negative) trends in SM, 3.57% (20.12%) was significant, respectively. The region located between 12°N to 20°N of latitude and 18°W to 18°E of longitude is dominated by a positive variation in SM.

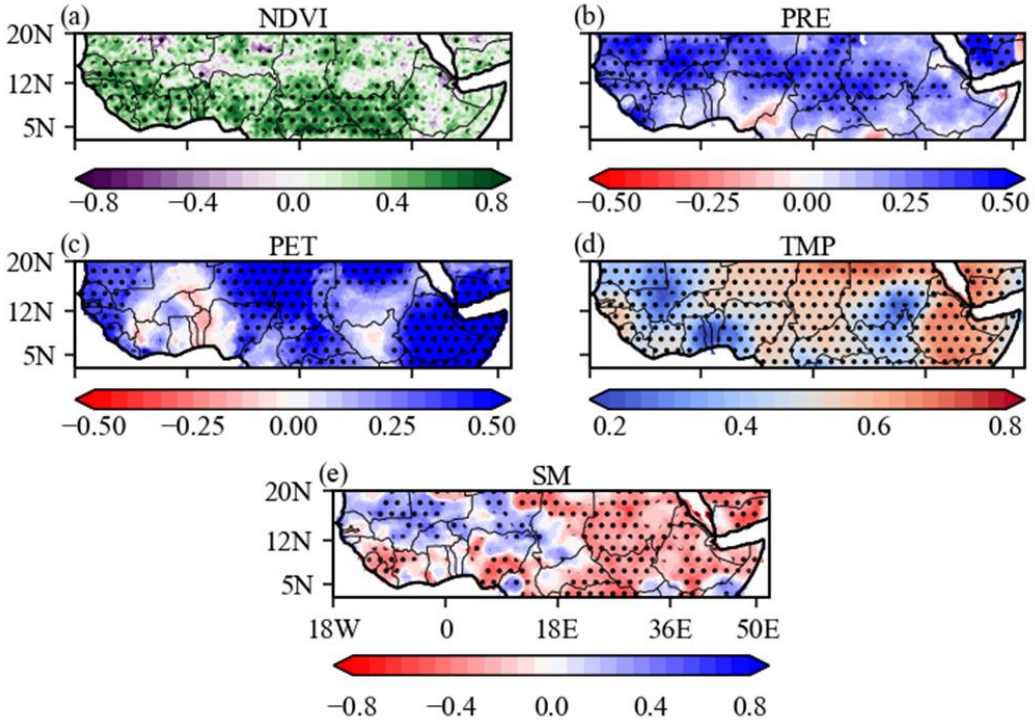

Fig. 6: Distribution of the MK trend for (a) NDVI, (b) PRE, (c) PET, (d) TMP and (e) SM over 1982–2015. The dots indicate significance at the 5% level.

3.5.Matrix correlation and collinearityvia variance inflation fractiontests of hydro-climatic drivers

The correlation matrix is used to evaluate the association between hydro-climatic factors as shown in Figure7. To check the multicollinearity between between the climate drivers, the matrix correlationand the variance inflation fraction (VIF) tests are used. A significant correlation (r = 0.83) is found between PET and TMP, it means that when the temperature increases, the potential evapotranspiration increases. Significant negative correlations of SM with PET and TMP are obtained i.e., when temperature increases, the soil moisture decreases through the increase of potential evapotranspiration.

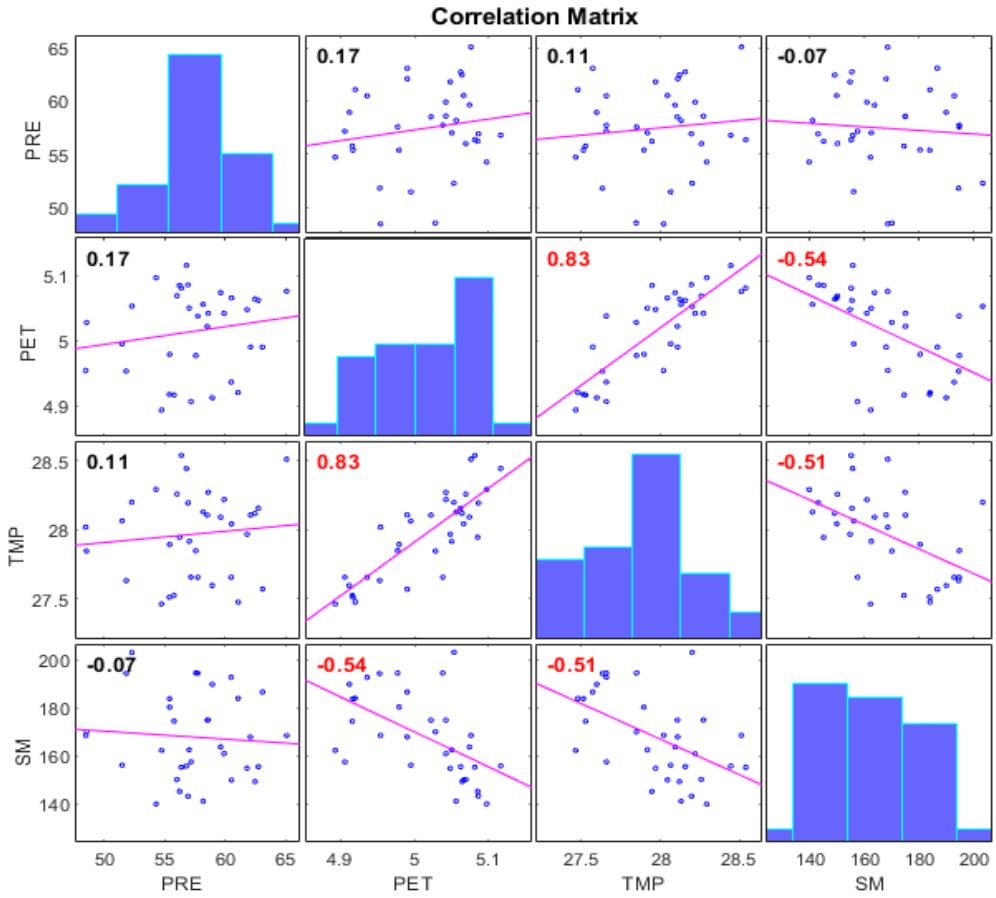

Fig. 7: Matrix Correlation between hydro-climatic factors. Units: PRE (mm), PET (mm day^{-1}), TMP (°C) and SM (mm). The values in red indicate significance at the 5% level.

The VIF test shows TMP and PET have high values (greater than 3), respectively. The combination of the correlation coefficient and that of VIF indicated a slight collinearity between variable TMP and PET. The VIF test for the variables PRE, TMP and SM is reconducted and it showed low values (less or equal to 1.4). Hence, the variable PET is eliminated in the afterwards of the study for enhancementof the consistency of relationships between hydro-climatic drivers and NDVI.

3.6.Relationships between single hydro-climatic factors and NDVI classes

The relationship between hydroclimatic factors and annual average NDVI and the time series of each NDVI class is assessed based on the equation (4).

The association of the climate factors (PRE, TMP, and SM) with each class of the NDVI (LVC, MVC, HVC, VVC, and EVC) was examined (Table 3) during 1982–2015. We have approximated the hydro-climatic factor time series of the area corresponding with each NDVI

class. A positive correlation between PRE and EVC was obtained, which was not significant at the 5% level. However, negative associations of PRE with LVC, MVC, HVC, and VVC wereobtained, respectively. Among these NDVI classes, the LVC was the sole class that was highly linked to the precipitation anomaly. The increase of precipitation was associated with a significant decrease in LVC but a weak decrease trend in moderate, high, and very high vegetation cover during the study period. The very high ecosystem class increased when precipitation increased. The growth of the EVC class was somehow dependent on the precipitation. Meanwhile, the precipitation played a reduced role for LVC, low, moderate, and high vegetation cover.

A non-significant negative correlation between TMP and EVC was obtained. The negative connection of TMP with EVC suggested that a decrease in TMP followed an increase in EVC. The rise in temperature was not beneficial for very high vegetation in NSSA. However, a positive association of TMP with LVC, MVC, HVC, and VVC during 1982–2015 was revealed. This signified that influences of TMP on LVC, MVC, and HVC ecosystem classes were weak though positive. Besides, the interaction of TMP with VVC was significant. The growth of high vegetation was dependent on the rising of temperature.

The vegetation coverage such as the LVC, MVC, and EVC classes was negatively linked to SM. The negative linkage coefficient meant that an increase in SM led to a decrease in low, moderate, and extreme vegetation cover. Elevated soil moisture reduced the development of these vegetation classes. Nevertheless, the ecosystem classes such as HVC and VVC were weakly and positively associated with SM. Values indicated the positive relationship of SM with HVC and VVC. That meant that an increase in SM is related to a weak increase in moderate and high vegetation categories.

3.7.Relationships between single hydro-climatic variables and NDVI

On one hand, the connections between area average time series of NDVI and precipitation, temperature and soil moisture are assessed on the one hand (Figure 8). The slope change rate of the NDVI during anomalous PRE, TMP and SM is 0.0014 mm $year^{-1}$, 0.0098°C $year^{-1}$ and −0.0001 mm $year^{-1}$, respectively. Statistically significant correlation coefficient at the 5% level is found between NDVI and PRE and TMP. Thus, the area average precipitation and temperature are indicators of positive change in area average NDVI.

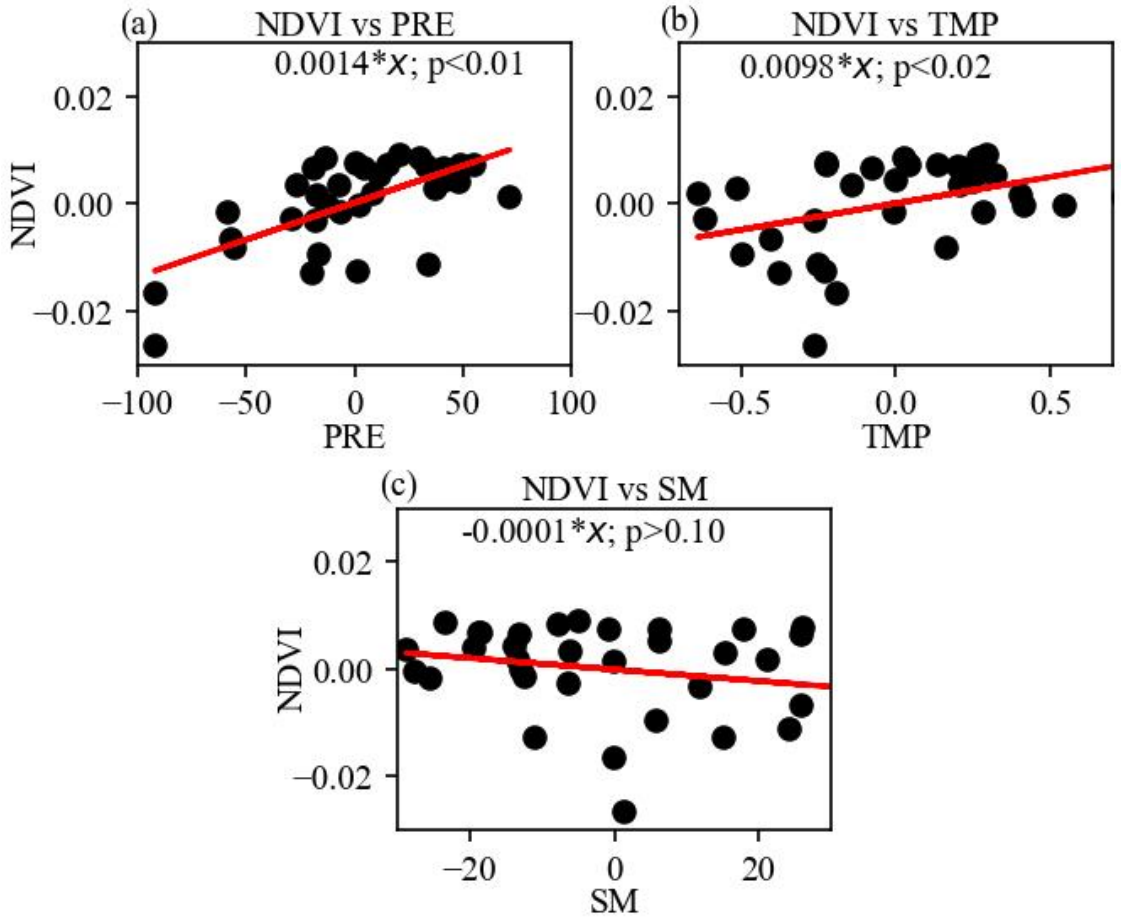

411

412 **Fig. 8** : Scatter plots of area-averaged NDVI with (a) PRE, (b) TMP and (c) SM for the period
413 from 1982 to 2015. The points represent area-averaged values of each parameter.

414 On the second hand, point-to-point correlationwere examined and presented in Figure 9.
415 Positive and negative correlations coefficient between NDVI and PRE, TMP and SM are found.
416 The areas that experienced positive (negative) correlation between PRE and NDVI occupied
417 23.73% (48.83%). Significant positive (negative) at the 5% level of these correlations occupied
418 1.67% (11.59%). Positive (negative) correlations of NDVI with TMP occupied 15.22% (57.60%)
419 of the total area, while significant positive (negative) correlations at the 5% level exhibited
420 3.37%(26.19%) of it. The area that experienced positive (negative) correlation between SM and
421 NDVI occupied 42.91% (41.04%). Significant positive (negative) correlations at the 5% level
422 occupied 10.24% (6.75%). Somehow, the precipitation, temperature and soil moisture contributed
423 differently to the variation of NDVI.

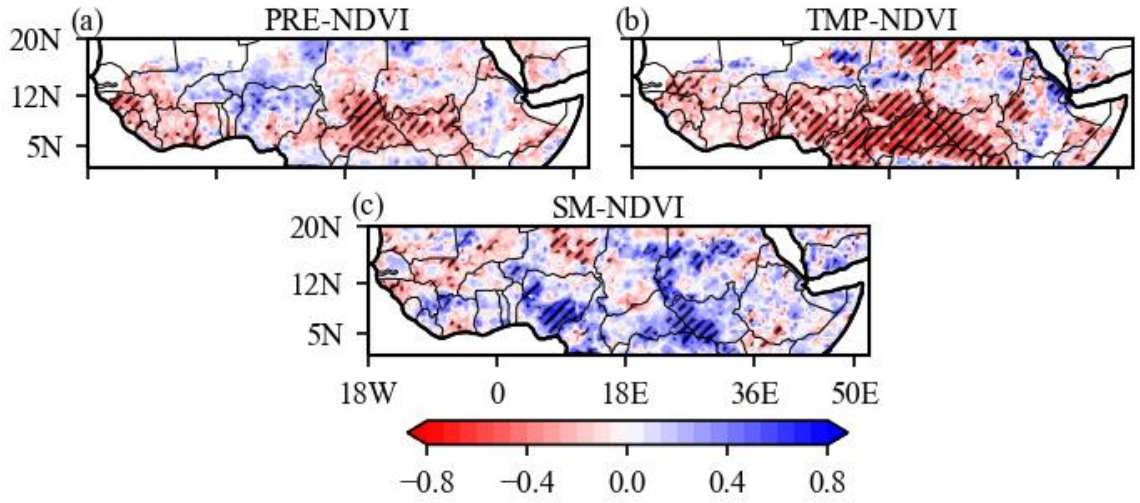

Fig. 9 : Spatial distribution of correlations coefficients of NDVI with (a) PRE, (b) TMP and (c) SM for the period from 1982–2015. The hatches represent significant at the 5% level.

3.8.Multiple regression of hydro-climatic divers on NDVI

Pixels based values of the dependent and independents variables were used to evaluate the relationship between their variations (Figure10 (a)). This analysis did not intend to predict, but to appraise the linkage between climate drivers and NDVI anomlies. A statistically significant relationship is obtained between hydro-climaticdrivers with NDVI anomalies. Positive (negative) anomalies of NDVI over the GC (NS and ES) were associated with hydro-climaticfactors respectively.

The area-averaged of the dependent and independent variables are used (Figure 10 (b)). The combination of the climate drivers such as PRE, TMP and SM showed significant relationship with NDVI over the 34 years ($r^2 = 0.491$, $p < 0.01$). However, the SM plays a negative role while the PRE and TMP play positive influence on NDVI with slope change of -0.0900 year^{-1} ($p > 0.6$), 0.5819 year^{-1} ($p < 0.01$) and 0.4274 year^{-1} ($p < 0.10$), respectively. We also, considered removing TMP to comprehend whether PRE and SM are sufficient enough to assess the relationship between NDVI and climate drivers. The result showed that the combination of the PRE, TMP and SM paremeters are better than considering two parameters (PRE and TMP). For illustration, the regression based on a single driver of NDVI change showed PRE ($r = 0.5849$, $p < 0.01$) and TMP ($r = 0.3542$, $p < 0.01$).

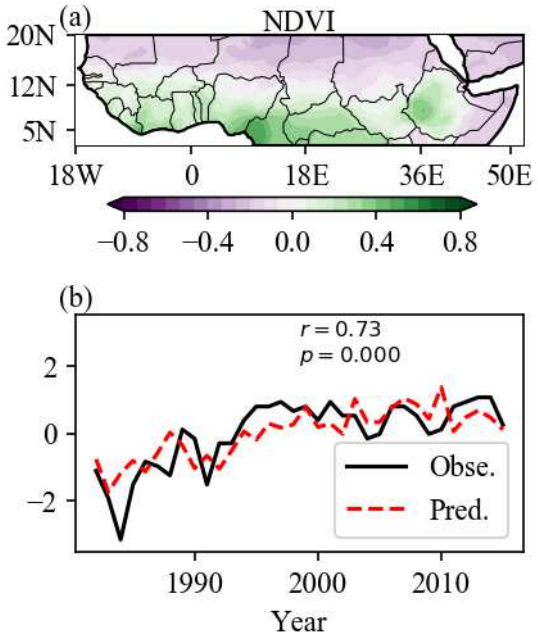

Fig. 10: (a) Spatial distribution of the relationship of NDVI anomalies and (b) area-averaged time series hydro-climatic drivers.

3.9.Multiple regression of hydro-climatic divers on NDVI classes

The hydro-climate drivers showed a significant association with LVC. The precipitation (r = −0.1648, p = 0.274) and soil moisture (r = −0.4055, p = 0.023) are negatively correlated with the LVC whereas its is positively correlated with the temperature (r = 0.0848, p > 0.10). When the precipitation and soil moisture increase, the low vegetation cover decreases. This could be explained by the fact these vegetation types are sensitive to a high-amount of water. The positive association of LVC with temperature means that increase in temperature will lead to increase in evaporation hence reduce of the soil water content. The predicted NDVI and original NDVI showed significant relationship with r = 0.47 and p = 0.005. However, when suppressing the temperature, the confidence level of association between the predicted and original NDVI was reduced, this means that the combination of climate factors is preferred to predicting the low vegetation cover than using a single variable.

The hydro-climatic drivers (r^2 = 0.041, p = 0.738) are non-significantly associated with the MVC. PRE (r = −0.1090, p = 0.574) and TMP (r = −0.1388, p = 0.530) are negatively correlated with MVC, whereas SM (r = 0.0219, p = 0.912) is positively associated with it. The increase of

463 soil moisture resulted in increase of the medium vegetation cover. This means that the soil moisture
464 is a limiting factor for the medium vegetation cover.

465 The HVC showed a significant relation with climate factors with an $r^2 = 0.225$ and $p =$
466 0.0508). Meanwhile, PRE ($r = -0.1648$, $p = 0.274$) and SM ($r = -0.4055$, $p = 0.023$) are negatively
467 correlated with HVC, whereas TMP is positively correlated with HVC ($r = 0.0848$, $p = 0.638$).

468 Hydro-climatic drivers are not significantly associated with VVC in view of the $r^2 = 0.159$
469 with $p = 0.151$. A non-significant but positive relationship is observed between VVC and TMP
470 and SM. At this time, the TMP is significantly correlated with VVC ($r = 0.4482$, $p = 0.053$) at the
471 5% level, suggesting that temperature was an indicator of very high vegetation cover. However,
472 the PRE is negatively connected with VVC, which is not statistically significant. It means that an
473 increase of the precipitation is associated with a decreasing of the very high vegetation cover.

474 EVC is negatively associated with SM ($r = -0.2275$, $p = 0.316$) and TMP ($r = -0.0558$, p
475 $= 0.815$), whereas the PRE ($r = 0.0037$, $p = 0.984$) is positively associated with EVC. Overall, the
476 EVC is not significantly related with these hydro-climatic drivers because $r^2 = 0.040$ and $p = 0.741$.
477 The extreme high vegetation cover increase when soil moisture and temperature decrease whereas
478 an increase in it is associated with increase in precipitation. A continuous increasing in temperature
479 as result of climate change, is desastratous for certain categories of plants.

480 **4. Discussions**

481 The paper reviews the recent change in hydro-climatic variables over the NSSA for the period
482 1982–2015 using the Mann-Kendall test, simple linear regression and multiple regression analyses.
483 It assesses the relationship of the hydro-climatic variables with the variations in the vegetation
484 cover using the NDVI as proxy data. To the extent of our knowledge, the temperature and the
485 potential evapotranspiration received less attention particularly in views of their relationship with
486 NDVI. The findings of the study indicated that the area-averaged NDVI at regional and sub-
487 regional scales over the period of study significantly increased. The increase of NDVI found is in
488 agreement with previous studies over the region (e.g., Hänke et al., 2016). However, previous work
489 did not pay attention to the categories of NDVI that contributed to the greening of Sahel despite
490 browing of vegetation cover could be observed over parts of the NSSA. A study demonstrated that
491 over Niger and Mali, some locations experienced negative change in vegetation, whereas others
492 experienced positive change in vegetation (Dardel et al., 2014). According to this analysis, the

greening of NSSA would be attributed to positive change in the low vegetation cover, very high vegetation cover and extreme high vegetation cover. Meanwhile, the medium vegetation cover, high vegetation cover undergone a declining. The spatial distribution of trend in NDVI showed an heterogeneous changes. The reverse change observed at patial scale could be explained by the medium and high vegetation cover.

The NSSA experienced increases in PRE, TMP and PET, but dominated by a declining trend in SM. The increase obtained for PRE and TMP are consistent with many studies conducted over the region(Collins, 2011; Ogou et al., 2019).The atmospheric ciruculation contributed to the increase in PRE (Sindikubwabo et al., 2018). It is worth noting that the PET has increased over most parts of the area, however received less attention of researcherscompare with PRE, TMP and SM. Meanwhile, the SM decrease over most parts of the region. The decrease in SM could be explained by the high potential evapotranspiration under the effect of increase in temperature, which lead to a probable increase in precipitation.

The assessment of the relationship between the vegetation cover (NDVI) and hydro-climatic variables showed that the area-averaged NDVI is positive and significantly correlated with the area-averaged PRE and TMP, implying that they played (PRE and TMP) important roles in the growth ofvegetation cover. However, point-to-point correlations between NDVI and hydro-climatic variables depicted a dominant positive association between NDVI and SM. This showed that the soil moisture rather plays the control factor. The negative correlation obtained between PRE and NDVI over parts of NSSA region could be explained by the influence of human activities.For example, human activities such as expansions of agricultural areas and ubarnization would have contributed negativelyto the change in NDVI, although the precipitation had increased. It could also be explained by a decreasing in water use efficiency of certain categories of plants. It means that some plants are water tolerant while others non-water tolerant. The results of the area-averaged could be different that point-to-point analyses because of the values at a particular site (grid-point) could be minimized or maximizedby that of other sites.

The multiple regression of hydro-climatic drivers effect on NDVI showed that area-averaged soil moisture is negatively associated with positive vegetation cover changes, but the PRE and TMP are significantly and positively associated with positive change in vegetation cover. This confirm the result of single relationship assessment. Based on temporal relationship, it is found that PRE and TMP are contributing factors locally to the increasing trend of NDVI over the NSSA.

The TMP considered in the current analysis had not been previously taken into account, thoughstudies had emphasized the warming of the region probably as the result of climate change.The temperature was likely to control the low vegetation cover and high vegetation cover, whilethe soil moisture controlled the growth of the medium vegetation cover.Meanwhile, the precipitation controlled the high vegetation cover and altogetherprecipitation, soil moisture and temperature controlled very high vegetation cover with stronger relation with the temperature. The different reactions of the vegetation cover (NDVI) to the soil moisture could be due the depth at which the water is available for roots of each category of plants.

The pixels based evaluation showed that soil moisture is the most prominent factor of the vegetation cover. It is worth noting that the simultaneous effect of three hydro-climatic factors is likely to be more useful for monitoring and predicting of vegetation cover over the NSSA.These findings are important for environmental monitoring and policy making for the land cover both at regional and local scales.

5. Conclusion

The vegetation cover through the use of NDVI and hydro-climatic variables were analysed for the period 1982-2015 over northern Sub-Saharan Africa (NSSA). The trends in hydro-climatic variables and NDVI were studied. NDVI classes and trends were also computed and the relation between the NDVI classes and hydro-climatic variables were also examined. The trend analysis showed that precipitation, temperature and potential evapotranspiration and NDVI had increased during 1982-2015.

The Classification of the vegetation cover using NDVI showed that the region is dominated by the low vegetation with approximately an area coverge of 37%. Types of vegetation cover had increased when others had decreased of the 34 years. Different classes of NDVI was associated differently with hydro-climatic factors.

The temporal relationship showed a significant association of the NDVI with PRE and TMP. The temperature was revealed to be an important factor as well for the vegetation cover change over the NSSA, which may be resulted from the global warming effect. Meanwhile, the spatial distribution depicted the SM as the factor contributing to the greening of the region.

The multiple regression showed that spatially, the soil moisture is the most contributor to the greening of NSSA though the contribution from TMP and PRE were also significant, which

consistent with previous studies showing that not only the precipitation or soil moisture drived the greening over NSSA in recent decades. More studies are needed to comprehend better about the greening of this region.

Acknowledgments

We sincerely thank CAS-TWAS and the UCAS for their support during our Ph.D. program. We also appreciate the World Meteorological Organization (WMO) for their support, which allowed us to study in this field.

Funding

There is no funding available for this research work.

Ethics Declarations

Ethical Approval

We the undersigned declare that this manuscript is original, has not been published before and is not under consideration for publication elsewhere.

Consent to participate

Not applicable

Conflict of Interest

Authors declare no conflict of interest.

Consent for publication

All authors consented to pubish the manuscript

Data Availability

All the data used in the work are available in the public domain and can be freely downloaded at the the links provided in the manuscript.

Code Availability

Code is freely available from corresponding author upon request.

Author Contribution

Conceptualization: Faustin Katchele Ogou; Methodology: Faustin Katchele Ogou; Data Analysis and Draft: Faustin Katchele Ogou and Tertsea Igbawua; Original Manuscript draft: Faustin Katchele Ogou; Supervision and review: Tertsea Igbawua

References

Abdi, A.M., Seaquist, J., Tenenbaum, D.E., Eklundh, L., Ardö, J., 2014. The supply and demand of net primary production in the Sahel. Environ. Res. Lett. 9. https://doi.org/10.1088/1748-9326/9/9/094003

Aklesso, M., Kumar, K.R., Bu, L., Boiyo, R., 2018. Analysis of spatial-temporal heterogeneity in remotely sensed aerosol properties observed during 2005–2015 over three countries along the Gulf of Guinea Coast in Southern West Africa. Atmos. Environ. 182, 313–324. https://doi.org/10.1016/j.atmosenv.2018.03.062

Bachelet, D., Neilson, R.P., Lenihan, J.M., Drapek, R.J., 2001. Climate change effects on vegetation distribution and carbon budget in the United States. Ecosystems 4, 164–185. https://doi.org/10.1007/s10021-001-0002-7

Barbosa, H.A., Huete, A.R., Baethgen, W.E., 2006. A 20-year study of NDVI variability over the Northeast Region of Brazil. J. Arid Environ. 67, 288–307. https://doi.org/10.1016/j.jaridenv.2006.02.022

Bégué, A., Vintrou, E., Ruelland, D., Claden, M., Dessay, N., 2011. Can a 25-year trend in Soudano-Sahelian vegetation dynamics be interpreted in terms of land use change? A remote sensing approach. Glob. Environ. Chang. 21, 413–420. https://doi.org/10.1016/j.gloenvcha.2011.02.002

Brandt, M., Hiernaux, P., Rasmussen, K., Mbow, C., Kergoat, L., Tagesson, T., Ibrahim, Y.Z., Wélé, A., Tucker, C.J., Fensholt, R., 2016. Assessing woody vegetation trends in Sahelian drylands using MODIS based seasonal metrics. Remote Sens. Environ. 183, 215–225. https://doi.org/10.1016/j.rse.2016.05.027

Chou, C., Huang, L.-F., Tseng, L., Tu, J.-Y., Tan, P.-H., 2009. Annual Cycle of Rainfall in the Western North Pacific and East Asian Sector. J. Clim. 22, 2073–2094.

https://doi.org/10.1175/2008JCLI2538.1

Collins, J.M., 2011. Temperature variability over Africa. J. Clim. 24, 3649–3666. https://doi.org/10.1175/2011JCLI3753.1

Dardel, C., Kergoat, L., Hiernaux, P., Mougin, E., Grippa, M., Tucker, C.J., 2014. Re-greening Sahel: 30 years of remote sensing data and field observations (Mali, Niger). Remote Sens. Environ. 140, 350–364. https://doi.org/10.1016/j.rse.2013.09.011

Dool, H.V.D., 2003. Performance and analysis of the constructed analogue method applied to U.S. soil moisture over 1981–2001. J. Geophys. Res. 108, 1–16. https://doi.org/10.1029/2002jd003114

Eklundh, L., Olsson, L., 2003. Vegetation index trends for the African Sahel 1982-1999. Geophys. Res. Lett. 30, 1–4. https://doi.org/10.1029/2002GL016772

Fensholt, R., Proud, S.R., 2012. Evaluation of Earth Observation based global long term vegetation trends - Comparing GIMMS and MODIS global NDVI time series. Remote Sens. Environ. 119, 131–147. https://doi.org/10.1016/j.rse.2011.12.015

Gilbert, R.O., 1987. Statistical Methods for Environmental Pollution Monitoring, Wiley. ed. New York.

Gu, Z., Duan, X., Shi, Y., Li, Y., Pan, X., 2018. Spatiotemporal variation in vegetation coverage and its response to climatic factors in the Red River Basin, China. Ecol. Indic. 93, 54–64. https://doi.org/10.1016/j.ecolind.2018.04.033

Hänke, H., Börjeson, L., Hylander, K., Enfors-Kautsky, E., 2016. Drought tolerant species dominate as rainfall and tree cover returns in the West African Sahel. Land use policy 59, 111–120. https://doi.org/10.1016/j.landusepol.2016.08.023

Harris, I., Jones, P.D., Osborn, T.J., Lister, D.H., 2014. Updated high-resolution grids of monthly climatic observations - the CRU TS3.10 Dataset. Int. J. Climatol. 34, 623–642. https://doi.org/10.1002/joc.3711

Herrmann, S.M., Anyamba, A., Tucker, C.J., 2005. Recent trends in vegetation dynamics in the African Sahel and their relationship to climate. Glob. Environ. Chang. 15, 394–404.

https://doi.org/10.1016/j.gloenvcha.2005.08.004

Hoscilo, A., Balzter, H., Bartholomé, E., Boschetti, M., Brivio, P.A., Brink, A., Clerici, M., Pekel, J.F., 2015. A conceptual model for assessing rainfall and vegetation trends in sub-Saharan Africa from satellite data. Int. J. Climatol. 35, 3582–3592. https://doi.org/10.1002/joc.4231

Igbawua, T., Zhang, J., Chang, Q., Yao, F., 2016. Vegetation dynamics in relation with climate over Nigeria from 1982 to 2011. Environ. Earth Sci. 75. https://doi.org/10.1007/s12665-015-5106-z

Jones, P.D., Hulme, M., 1996. Calculating regional climatic time series for temperature and precipitation: methods and illustrations. Int. J. Climatol. 16, 361–377. https://doi.org/10.1002/(SICI)1097-0088(199604)16:4<361::AID-JOC53>3.0.CO;2-F

Karlson, M., Ostwald, M., 2016. Remote sensing of vegetation in the Sudano-Sahelian zone: A literature review from 1975 to 2014. J. Arid Environ. 124, 257–269. https://doi.org/10.1016/j.jaridenv.2015.08.022

Kaspersen, P.S., Fensholt, R., Huber, S., 2011. A spatiotemporal analysis of climatic drivers for observed changes in Sahelian vegetation productivity (1982-2007). Int. J. Geophys. 2011. https://doi.org/10.1155/2011/715321

Kendall, M.G., 1975. Rank correlation methods., Griffin. ed. London.

Leroux, L., Bégué, A., Lo Seen, D., Jolivot, A., Kayitakire, F., 2017. Driving forces of recent vegetation changes in the Sahel: Lessons learned from regional and local level analyses. Remote Sens. Environ. 191, 38–54. https://doi.org/10.1016/j.rse.2017.01.014

Los, S.O., 2013. Analysis of trends in fused AVHRR and MODIS NDVI data for 1982-2006: Indication for a CO 2 fertilization effect in global vegetation. Global Biogeochem. Cycles 27, 318–330. https://doi.org/10.1002/gbc.20027

Lukamba, M., 2010. Natural disasters in African countries: what can we learn about them? J. Transdiscipl. Res. South. Africa 6, 478–495.

Mann, H.B., 1945. Non-parametric test against trend. Econometrica 13, 245–259.

663 Mulugeta, M., Tolossa, D., Abebe, G., 2017. Data in Brief Description of long-term climate data
664 in Eastern and Southeastern Ethiopia. Data Br. 12, 26–36.
665 https://doi.org/10.1016/j.dib.2017.03.025

666 Nicholson, S.E., 2000. The nature of rainfall variability over Africa on times scales of decades to
667 millennia. Glob. Planet. Change 26, 137–158.

668 Nicholson, S.E., 1980. The Nature of Rainfall Fluctuations in Subtropical West Africa. Mon.
669 Weather Rev. 108, 473–487. https://doi.org/10.1175/1520-
670 0493(1980)108<0473:TNORFI>2.0.CO;2

671 Nicholson, S.E., Farrar, T.J., 1994. The influence of soil type on the relationships between
672 NDVI, rainfall, and soil moisture in semiarid Botswana. I. NDVI response to rainfall.
673 Remote Sens. Environ. 50, 107–120. https://doi.org/10.1016/0034-4257(94)90038-8

674 Nicholson, S.E., Kim, J., 1997. the Relationship of the El Niño–Southern Oscillation To African
675 Rainfall. Int. J. Climatol. 17, 117–135. https://doi.org/10.1002/(SICI)1097-
676 0088(199702)17:2<117::AID-JOC84>3.0.CO;2-O

677 Ogou, F.K., Yang, Q., Duan, Y., Ma, Z.Z.-G., 2019. Comparative analysis of interdecadal
678 precipitation variability over central North China and sub Saharan Africa. Atmos. Ocean.
679 Sci. Lett. 12, 1–7. https://doi.org/10.1080/16742834.2019.1593040

680 Okoro, U.K., Chen, W., Chineke, C., Nwofor, O., 2017. Anomalous Atmospheric Circulation
681 Associated with Recent West African Monsoon Rainfall Variability 1–27.
682 https://doi.org/10.4236/gep.2017.512001

683 Olsson, L., Eklundh, L., Ardö, J., 2005. A recent greening of the Sahel - Trends, patterns and
684 potential causes. J. Arid Environ. 63, 556–566.
685 https://doi.org/10.1016/j.jaridenv.2005.03.008

686 Pei, F., Wu, C., Liu, X., Li, X., Yang, K., Zhou, Y., Wang, K., Xu, L., Xia, G., 2018. Monitoring
687 the vegetation activity in China using vegetation health indices. Agric. For. Meteorol. 248,
688 215–227. https://doi.org/10.1016/j.agrformet.2017.10.001

689 Peng, W., Kuang, T., Tao, S., 2019. Quantifying influences of natural factors on vegetation
690 NDVI changes based on geographical detector in Sichuan, western China. J. Clean. Prod.

233, 353–367. https://doi.org/10.1016/j.jclepro.2019.05.355

Philippon, N., Jarlan, L., Martiny, N., Camberlin, P., Mougin, E., 2007. Characterization of the interannual and intraseasonal variability of West African vegetation between 1982 and 2002 by means of NOAA AVHRR NDVI data. J. Clim. 20, 1202–1218. https://doi.org/10.1175/JCLI4067.1

Pinzon, J.E., Brown, M.E., Tucker, C.J., 2005. Hilbert-Huang transform and its applications., N.E. Huang. ed. Singapore; Hackensack, NJ; London: World Scientific. https://doi.org/https://doi.org/10.1142/5862

Pinzon, J.E., Tucker, C.J., 2014. A non-stationary 1981-2012 AVHRR NDVI3g time series. Remote Sens. 6, 6929–6960. https://doi.org/10.3390/rs6086929

Pravalie, R., Sîrodoev, I., Peptenatu, D., 2014. Detecting climate change effects on forest ecosystems in Southwestern Romania using Landsat TM NDVI data. J. Geogr. Sci. 24, 815–832. https://doi.org/10.1007/s11442-014-1122-2

Schlenker, W., Lobell, D.B., 2010. Robust negative impacts of climate change on African agriculture. Environ. Res. Lett. 5. https://doi.org/10.1088/1748-9326/5/1/014010

Sen, P.K., 1968. Estimates of the Regression Coefficient Based on Kendall's Tau. J. Am. Stat. Assoc. 63, 1379–1389. https://doi.org/10.1080/01621459.1968.10480934

Sindikubwabo, C., Li, R., Wang, C., 2018. Abrupt Change in Sahara Precipitation and the Associated Circulation Patterns. Atmos. Clim. Sci. 08, 262–273. https://doi.org/10.4236/acs.2018.82017

Spiekermann, R., Brandt, M., Samimi, C., 2015. Woody vegetation and land cover changes in the Sahel of Mali(1967-2011). Int. J. Appl. Earth Obs. Geoinf. 34, 113–121. https://doi.org/10.1016/j.jag.2014.08.007

Swaine, M.D., 1992. Characteristics of dry forest in West Africa and the influence of fire. J. Veg. Sci. 3, 365–374.

Traore, S.B., Ali, A., Tinni, S.H., Samake, M., Garba, I., Maigari, I., Alhassane, A., Samba, A., Diao, M.B., Atta, S., Dieye, P.O., Nacro, H.B., Bouafou, K.G.M., 2014. AGRHYMET: A

718 drought monitoring and capacity building center in the West Africa Region. Weather Clim.
719 Extrem. 3, 22–30. https://doi.org/10.1016/j.wace.2014.03.008

720 Tucker, C.I., 1986. Maximum normalized difference vegetation index images for subSaharan
721 Africa for 1983-1985. Int. J. remoyte Sens. 7, 1383–1384.

722 Vlek, P., Le, Q.B., Tamene, L., 2008. Land decline in Land-Rich Africa– A creeping disaster in
723 the making. Rome, Italy:

724 Wagner, R.G., da Silva, A.M., 1994. Surface conditions associated with anomalous rainfall in the
725 guinea coastal region. Int. J. Climatol. 14, 179–199. https://doi.org/10.1002/joc.3370140205

726 Xu, Y., Yang, J., Chen, Y., 2016. NDVI-based vegetation responses to climate change in an arid
727 area of China. Theor. Appl. Climatol. 126, 213–222. https://doi.org/10.1007/s00704-015-
728 1572-1

729 Yang, W., Seager, R., Cane, M., Lyon, B., 2013. The East African Long Rains in Observations
730 and Models. https://doi.org/10.13140/2.1.2461.3443

731 Yang, W., Seager, R., Cane, M.A., Lyon, B., 2015. The Annual Cycle of East African
732 Precipitation. J. Clim. 28, 2385–2404. https://doi.org/10.1175/JCLI-D-14-00484.1

733 Yang, Y., Wang, S., Bai, X., Tan, Q., Li, Q., Wu, L., Tian, S., Hu, Z., Li, C., Deng, Y., 2019.
734 Factors affecting long-term trends in global NDVI. Forests 10, 1–17.
735 https://doi.org/10.3390/f10050372

736 Zewdie, W., Csaplovics, E., Inostroza, L., 2017. Monitoring ecosystem dynamics in
737 northwestern Ethiopia using NDVI and climate variables to assess long term trends in
738 dryland vegetation variability. Appl. Geogr. 79, 167–178.
739 https://doi.org/10.1016/j.apgeog.2016.12.019

740 Zhang, H., Chang, J., Zhang, L., Wang, Y., Li, Y., Wang, X. p., 2018. NDVI dynamic changes
741 and their relationship with meteorological factors and soil moisture. Environ. Earth Sci. 77,
742 1–11. https://doi.org/10.1007/s12665-018-7759-x

743 Zhang, X., Friedl, M.A., Schaaf, C.B., Strahler, A.H., Liu, Z., 2005. Monitoring the response of
744 vegetation phenology to precipitation in Africa by coupling MODIS and TRMM

instruments. J. Geophys. Res. D Atmos. 110, 1–14. https://doi.org/10.1029/2004JD005263

Zhang, X., Wu, S., Yan, X., Chen, Z., 2017. A global classification of vegetation based on NDVI, rainfall and temperature. Int. J. Climatol. 37, 2318–2324. https://doi.org/10.1002/joc.4847

Zhang, Y., Zhang, C., Wang, Z., Chen, Y., Gang, C., An, R., Li, J., 2016. Vegetation dynamics and its driving forces from climate change and human activities in the Three-River Source Region, China from 1982 to 2012. Sci. Total Environ. 563–564, 210–220. https://doi.org/10.1016/j.scitotenv.2016.03.223

Supplementary Files

This is a list of supplementary files associated with this preprint. Click to download.

- Supplementaryfile1.docx